

Investigating the Interaction of Crystal Violet Probe Molecules on Sodium Dodecyl Sulfate Micelles with Hyper-Rayleigh Scattering

Guillaume Revillod, Isabelle Russier-Antoine, Emmanuel Benichou, Christian Jonin, and Pierre-François Brevet*

Laboratoire de Spectrométrie Ionique et Moléculaire, UMR CNRS 5579, Université Claude Bernard Lyon 1, Bâtiment Alfred Kastler, 43 Boulevard du 11 Novembre 1918, 69622 Villeurbanne Cedex, France

Received: November 22, 2004; In Final Form: January 18, 2005

We report the use of the nonlinear optical technique of hyper-Rayleigh scattering to investigate the interaction of the cationic probe molecule crystal violet with micelles of sodium dodecyl sulfate. An absolute value of $(847 \pm 80) \times 10^{-30}$ esu is measured at the fundamental wavelength of 870 nm for the molecular hyperpolarizability of crystal violet free in pure aqueous solutions. In aqueous solutions of sodium dodecyl sulfate, above and below the critical micelle concentration, the measured hyperpolarizability of crystal violet is weaker than in the solution free of sodium dodecyl sulfate. From the comparison with linear optical photoabsorption spectroscopy data, this difference is attributed to electrostatic interactions between the cationic crystal violet molecules and the negatively charged sodium dodecyl sulfate surfactant molecules present in excess. Polarization resolved hyper-Rayleigh scattering measurements are then performed to show that, below and above the critical micelle concentration, crystal violet molecules also undergo symmetry changes upon interaction with sodium dodecyl sulfate. Above the critical micelle concentration, the minimum fraction of micelles interacting with at least one CV molecule is estimated. For instance, for a crystal violet aqueous concentration of 150 μ M, this fraction is larger than 7%.

Introduction

Self-assembly is a fundamental process in nature, a process essential to life. It also leads to the design of rich and diverse classes of materials differing by their composition, their size, or their shape. Many areas are extensively making use of these self-assembled systems: for instance, chemistry with the synthesis of nanoparticles in reverse micelles, drug delivery with encapsulation in vesicles, or surface science with self-assembled monolayers onto surfaces. As a result, there is a constant need for the development of techniques to investigate the fine molecular details of the structures and the mechanisms involved in their formation.

In nonlinear optics, it has been demonstrated in the past that assemblies of nonlinear optical (NLO) chromophores could lead to large enhancements of the nonlinear optical response. For example, in the process of second harmonic generation (SHG), a phenomenon whereby two photons at the fundamental frequency are converted into one photon at the harmonic frequency, the enhancement of the SHG response arises from the spatial correlation of the different NLO chromophores involved in the molecular system, resulting in an enhanced hyperpolarizability of the ensemble.^{1–3} One simple example is a polymer backbone with NLO chromophores rigidly tethered onto it.⁴ However, this spatial correlation in an assembly of NLO chromophores may yield a vanishing SHG response. In that latter case, the critical parameter is the characteristic size a of the assembly as compared to the wavelength of light λ . For very small ratios a/λ , no retardation effects occur, and the overall hyperpolarizability of the ensemble is just the tensorial sum of the hyperpolarizability of each element of the ensemble. The resulting SHG signal thus depends on the molecular arrangement

of the NLO chromophores. This response vanishes for a random arrangement or for one displaying a center of inversion. For ratios a/λ of the order of unity, retardation effects come into play, and the observation of strong SHG signals is possible for structures possessing a center of inversion. The latter case has been investigated in detail in the past for malachite green adsorbed at the surface of liposomes or polystyrene microspheres.^{5,6} More recently, this close relationship between the organization of the assembly and the magnitude of the SHG response has been used to determine the critical micelle concentration (cmc) of a surfactant solution.⁷ Indeed, a drop in the magnitude of the SHG intensity was observed as a function of the surfactant concentration and attributed to the formation of micelles. This conclusion obviously assumed that the micelles possessed a center of inversion and were much smaller than the wavelength of light.

Besides the problem of detecting nanometer scale molecular structures in a liquid solution, whether produced by self-assembly or any other methods, the investigation of the nature of these structures at the molecular level is also a challenge. Linear optical techniques do exist, for instance, static and dynamic light scattering. Photoabsorption and fluorescence spectroscopy are also useful techniques if the spectral properties of the molecular probe in the solution, entering or not a complex with the surfactant, change upon interaction with the assemblies. It is though not immediate to find techniques distinguishing probe molecules free in the surfactant solution and in interaction with micelles. In the case of the above-mentioned techniques, one would rely on the dynamics or the spectroscopic properties of the probe molecules to make the distinction. One may indeed assume that a probe molecule will not diffuse freely when interacting with a micelle or will have a different absorption spectrum or a different fluorescence depolarization ratio, proper-

* Corresponding author: Tel +33 (0) 472 445 873; Fax +33 (0) 472 445 871; e-mail pfbrevet@lasim.univ-lyon1.fr.

ties that can be addressed by dynamic light scattering, photoabsorption spectroscopy, or fluorescence depolarization. However, a major drawback is the partitioning of the probe molecules between different states, for instance freely dissolved in the solution, entering a complex with the surfactant or in interaction with the micelles. This partition often prevents a clear distinction between the different states.

We present here a nonlinear optical investigation, showing that the technique of hyper-Rayleigh scattering (HRS) may be used for this purpose. The changes of the hyperpolarizability tensor magnitude and the HRS depolarization ratio for crystal violet probe molecules free in solution, entering a complex with surfactant molecules and in interaction with sodium dodecyl sulfate (SDS) micelles are used to achieve this result. Crystal violet (CV) was used as the probe molecule because it has been extensively studied as a NLO chromophore with a large hyperpolarizability.⁸ Linear photoabsorption spectroscopy was also performed and compared to the nonlinear optical data obtained by HRS for the different states of the CV probe molecules.

Experimental Section

Nonlinear Optics. The hyper-Rayleigh scattering experimental setup was based on two different femtosecond Ti:sapphire oscillator laser sources. The first one was used for the HRS intensity measurements and provided pulses with a duration of about 70 fs and operated at a repetition rate of 80 MHz. The fundamental wavelength was set at 870 nm with an average power of 1.4 W. The second laser source was used for the polarization-resolved HRS measurements and provided pulses with a duration of about 150 fs and operated at a repetition rate of 76 MHz. The fundamental wavelength was set at 800 nm with an average power of 0.25 W. For both laser sources, the light beam was focused by a standard microscope objective onto a spectrophotometric quartz cell containing typically 3 mL of the aqueous solution. The second harmonic light was collected at a right angle through a 5 cm focal length lens into a monochromator. The signal was collected by a cooled photomultiplier tube feeding a photon counter. Color filters were placed on the fundamental and the harmonic light beam paths to avoid any unwanted SH or fundamental light. The spectrum of the fundamental light was measured to ensure that the pulse length was constant throughout the experiment. The laser beam was chopped at a fixed frequency to measure the noise level, and the measurement procedure was repeated several times. A half-wave plate defined the fundamental beam polarization state, and an analyzer defined the second harmonic light polarization state. All data were corrected for any laser power drifts.

Chemistry. Crystal violet (CV) (chloride salt) and sodium dodecyl sulfate (SDS) were used as received (Sigma Aldrich). All solutions were prepared from ultrapure water (Millipore).

Results and Discussion

CV Free in Solution. Crystal violet is a monocationic NLO chromophore that has been fully characterized in the past.^{8–10} Crystal violet has an octupolar molecular structure and a high hyperpolarizability, further enhanced when the harmonic frequency is in the vicinity of an electronic resonance. For example, at the fundamental wavelength of 800 nm, the hyperpolarizability of CV dissolved in methanol has been reported to be 450×10^{-30} esu.¹⁰ The photoabsorption spectrum of CV in aqueous solutions is reported in Figure 1. This spectrum presents two overlapping absorption bands in the range 500–600 nm. These two bands are thought to result from a solvent-induced

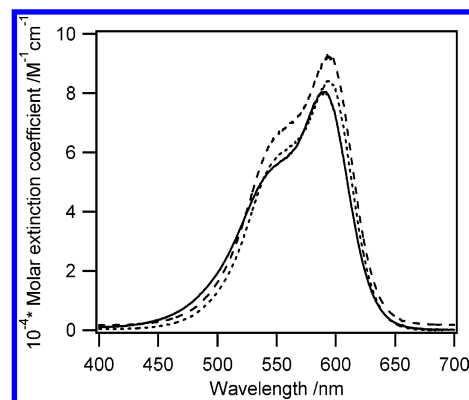


Figure 1. Molar extinction coefficient of crystal violet dissolved in pure water (solid), in 3.6 mM SDS aqueous solution (dotted), and in 33.6 mM SDS aqueous solution (dashed).

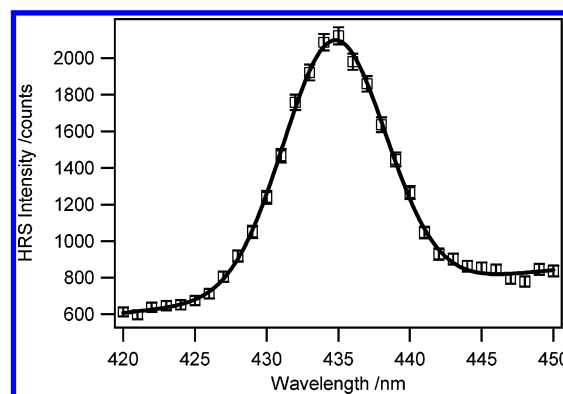


Figure 2. Hyper-Rayleigh scattering line for crystal violet dissolved in pure water at a concentration of 70 μM. The fundamental wavelength is 870 nm.

symmetry breaking of a degenerate excited state whereas the symmetry of the ground state is left unchanged. By successive dilutions of the aqueous solution of CV, an extinction coefficient of $80\,270 \pm 1140$ M⁻¹ cm⁻¹ at the maximum of absorption was determined for CV freely dissolved in water.

HRS measurements were then performed on pure aqueous solutions of CV for several concentrations, ranging from 50 up to 150 μM with a fundamental wavelength of 870 nm, in a region of a weak CV photoabsorption, as seen from Figure 1. The HRS intensity I_{HRS} collected at 435 nm is given by¹¹

$$I_{\text{HRS}} = G(N_S \langle \beta_S^2 \rangle + N_{\text{CV}}^0 \langle \beta_{\text{CV}}^2 \rangle) I^2 \exp(-\epsilon N_{\text{CV}}^0 l) \quad (1)$$

where G is a constant, I is the fundamental intensity, β_S and β_{CV} are the hyperpolarizability of the solvent and CV, respectively, N_S and N_{CV}^0 are the number density of the solvent and CV, respectively, ϵ is the molar extinction coefficient of CV at the harmonic wavelength, and l is the optical path length of the harmonic light in the cell. In all our measurements, water was used as the solvent. Here, it is assumed that at the fundamental frequency the absorption cross section vanishes. At high concentrations of CV, a weak self-absorption of the second harmonic (SH) light was observed and was well accounted for by the decreasing exponential factor present in eq 1. To ensure that an HRS signal was indeed observed, the HRS line itself was recorded by fixing the fundamental wavelength at 870 nm and scanning the monochromator from 420 up to 450 nm (see Figure 2). The HRS line peaked at 435 nm is then clearly observed sitting on a broad band background, as indicated by the nonvanishing signal levels measured at 420 and 450 nm. This background increases with the wavelength and is likely

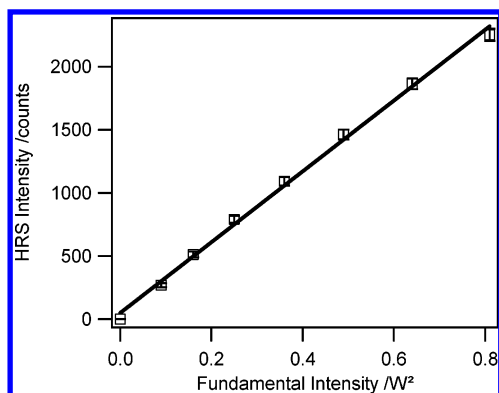


Figure 3. Dependence with the square of the fundamental intensity of the hyper-Rayleigh scattering intensity of crystal violet dissolved in pure water at a concentration of 70 μM .

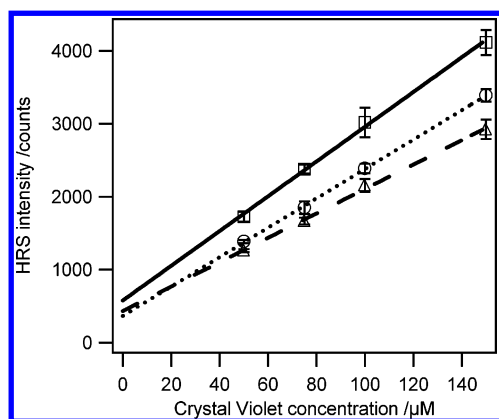


Figure 4. Dependence of the hyper-Rayleigh scattering intensity of crystal violet aqueous solutions for an SDS concentration of (solid) 0, (dotted) 3.6 mM, and (dashed) 33.6 mM.

the radiative decay from an excited state back to the ground state following a multiphoton excitation. Since this background does not vanish at shorter wavelength than the HRS line, the excitation process is likely, at least, a three-photon process.

Furthermore, the absorption band observed in Figure 1 is located on the red side of the HRS line, and therefore the maximum of the fluorescence band is expected at even longer wavelengths. Excitation from the ground state to the upper state can be a two-photon process since the absorption cross section is not strictly zero in the range 420–450 nm (see Figure 1), but a larger absorption cross section occurs for three and higher photon processes. Because of the occurrence of this background, all measurements of the HRS intensity entailed the recording of the HRS line and the subtraction of the background. This procedure was made possible by the incoherent nature of the HRS process. From the linear dependence of the HRS intensity with the square of the fundamental intensity (see Figure 3), it was concluded that the excited state did not play any significant role in the range studied, the hyperpolarizability being essentially that of the ground state. A similar conclusion was drawn at the wavelength of 800 nm.

Figure 4 presents the dependence of the HRS intensity with the CV concentration in SDS-free aqueous solutions. With the hyperpolarizability of neat water reported to be $\beta_s = 0.56 \times 10^{-30}$ esu, the magnitude of the hyperpolarizability tensor for CV in water at the fundamental wavelength of 870 nm was found to be $\beta = (874 \pm 80) \times 10^{-30}$ esu.¹² This latter value is in rather good agreement with previous data reported in the past.⁸ To complement the data, we also measured the depolarization ratio defined as the intensity collected for the harmonic

light vertically and horizontally polarized and the input fundamental light vertically polarized and compared it with theoretical calculations.¹³ This quantity is also obtained through the ratio of the intensity collected for the harmonic light vertically polarized and the fundamental light vertically and horizontally polarized. For a purely octupolar molecule like CV, the theoretical depolarization ratio defined as $D = \langle \beta_{CV,ZZX}^2 \rangle / \langle \beta_{CV,XXX}^2 \rangle$ is equal to 0.67, where the two elements of the molecular hyperpolarizability tensor β_{CV} are given in the laboratory frame. The theoretical depolarization ratio is thus in good agreement with the experimental value of 0.66 ± 0.02 . For a pure dipolar probe molecule, the theoretical depolarization ratio is 0.2 if there is only one nonvanishing hyperpolarizability tensor element. The element is simply β_{xxx} in the molecular frame where x is the charge-transfer 2-fold symmetry axis. However, if the other nonvanishing elements of the hyperpolarizability tensor are also taken into account, this depolarization ratio can take any value.¹⁴

CV in SDS-Containing Aqueous Solutions. SDS was used as the surfactant compound since its micellar properties are well-known. SDS forms micelles above an aqueous concentration of 8 mM, defined as the cmc, at 25 °C, and its aggregation number is 71. SDS is a sodium salt, and its sulfate polar head leads to negatively charged micelles. All aqueous concentrations used in these experiments of SDS were inferior to 50 mM, and therefore the micelles were assumed spherical with a mean diameter of about 3.5 nm.¹⁵ This diameter is much smaller than the fundamental wavelength of light used in these experiments, the value of which is either 870 or 800 nm. Below the cmc, SDS is freely dissolved in the solution. Above the cmc, two forms coexist: one is freely dissolved in the solution, and the other is involved in the micelles. The micelle concentration is thus simply $([\text{SDS}]_0 - \text{cmc})/71$, where $[\text{SDS}]_0$ is the total concentration of SDS. It was possible to record an HRS signal from the neat water solution and also from SDS aqueous solutions below and above the cmc. However, the HRS signals collected were small and identical in the three cases, leading to the conclusion that, subsequently, the SDS molecules were not directly detected.

In SDS-containing solutions, for SDS concentrations below the cmc, the photoabsorption spectrum of CV is slightly modified (see Figure 1). In particular, a small shift of the maximum of absorption of about 6 nm toward longer wavelengths is noticed with minimal change of the molar extinction coefficient, this latter coefficient being determined to be $83\,975 \pm 3090 \text{ M}^{-1} \text{ cm}^{-1}$ at the maximum of absorption. The change in the extinction coefficient upon introduction of SDS into the CV aqueous solution is therefore within the experimental error. The small shift of 6 nm toward long wavelengths is attributed to the electrostatic interactions of the cationic CV with the negatively charged SDS. Also reported in Figure 1 is the photoabsorption spectrum of CV in SDS-containing aqueous solutions above the cmc. The corresponding SDS concentration is 33.6 mM, well above the cmc, the value of which is only 8 mM. A clear increase of the extinction coefficient is observed, the value of which reaches $92\,400 \pm 1100 \text{ M}^{-1} \text{ cm}^{-1}$ at the maximum of absorption. However, no further shift of the maximum of absorption is observed. Again, these changes in the extinction coefficient are attributed to the interaction of CV with the micelles. At the harmonic wavelength of 435 nm, the shift of 6 nm to longer wavelengths of the maximum of the absorbance induces a weak decrease of the absorbance. Above the cmc, the absorbance is slightly increased to a value similar to the one obtained without SDS.

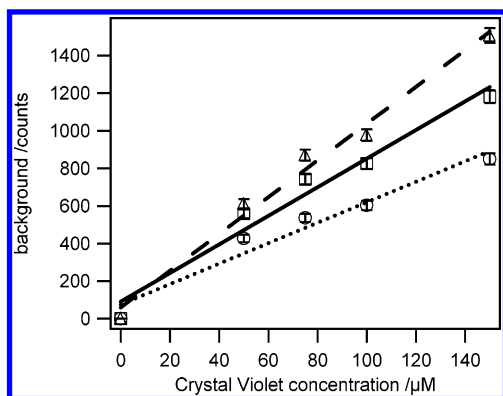


Figure 5. Dependence of the background signal interpolated at the hyper-Rayleigh scattering wavelength as a function of the crystal violet concentration of aqueous solutions for an SDS concentration of (solid) 0, (dotted) 3.6 mM, and (dashed) 33.6 mM.

Figure 4 gives the HRS intensity measured as a function of the CV concentration for SDS concentrations of 0, 3.6, and 33.6 mM. The HRS intensity measured at an SDS concentration above the cmc is weaker than the HRS intensity measured at an SDS concentration below the cmc, which is itself below the HRS intensity measured for the pure aqueous solutions of CV.

However, in all cases, the three curves can be fitted by linear fits with slopes of 1, 0.83, and 0.69 for SDS concentrations of 0, 3.6, and 33.6 mM, respectively. The slopes have been normalized to the slope of the linear fit obtained in the absence of any SDS. The intensity extrapolated at the origin for a vanishing CV concentration does not completely disappear, as expected. This is in agreement with the nonvanishing HRS intensity recorded for the pure aqueous solutions with or without SDS, below or above the cmc. The extrapolated HRS intensities for the neat water solution and the SDS containing solutions are all identical, the small differences arising from the background subtraction procedure. Figure 5 gives the fluorescence background signal, as determined at wavelengths away from the HRS line wavelength, below and above the HRS line, for the three different cases, namely 0, 3.6, and 33.6 mM SDS concentrations, and recalculated by linear interpolation at 435 nm.

As expected, this background signal is a linear function of the CV concentration with a vanishing value at zero CV concentration. This observation further supports the need for a careful subtraction procedure to remove this fluorescence background signal. To our sensitivity, the three HRS linear plots displayed in Figure 4 yield the same intensity at vanishing CV concentration. Using eq 1, the experimental data were fitted with the following expression for the linear fits, once the contribution from the solvent has been removed:

$$I_{\text{HRS}}(\text{CV}) = G^2(N_{\text{CV}}^{\text{free}}\langle\beta_{\text{CV}}^2\rangle + N_{\text{CV}}^{\text{c}}\langle\beta_{\text{CVc}}^2\rangle + N_{\text{CV}}^{\text{m}}\langle\beta_{\text{CVm}}^2\rangle) \quad (2)$$

where $N_{\text{CV}}^{\text{free}}$ is the number density of free CV molecules in solution, N_{CV}^{c} is the number density of CV molecules entering a complex with SDS surfactant molecules, and N_{CV}^{m} is the number density of CV molecules in interaction with the micelles. The following relationship is valid:

$$N_{\text{CV}}^0 = N_{\text{CV}}^{\text{free}} + N_{\text{CV}}^{\text{c}} + N_{\text{CV}}^{\text{m}} \quad (3)$$

where N_{CV}^0 is the total number density of CV molecules. Similarly, β_{CVc} , the hyperpolarizability of the CV–SDS complexes, and β_{CVm} , the hyperpolarizability of CV molecules in

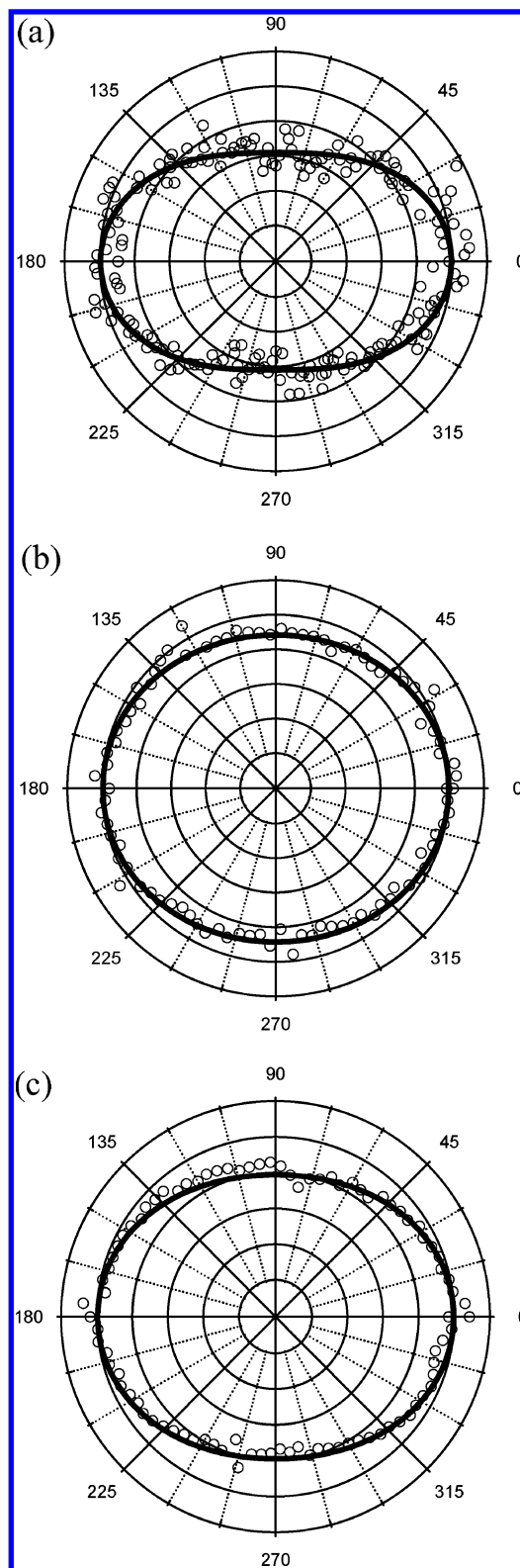


Figure 6. Polar plots of the HRS intensity vertically polarized as a function of the polarization angle of the fundamental beam for a 150 μM CV aqueous solution for the three cases: (a) free SDS solution, (b) SDS concentration below the cmc, and (c) SDS concentration above the cmc.

interaction with a micelle, have been introduced. In eq 2 and subsequently, all the hyperpolarizability elements are expressed in the macroscopic laboratory frame. In all experiments, the CV concentration never exceeded 150 μM . Thus, SDS was always in excess with its concentration being either 3.6 or 33.6 mM. Furthermore, the exact stoichiometry of the CV–SDS

complexes is not known. If the ratio $K = [\text{CV} + \text{SDS}]/[\text{CV}]$ between the CV molecules free in solution and in the CV–SDS complexes is introduced, the HRS intensity $I_{\text{HRS}}(\text{CV})$ is rewritten as

$$I_{\text{HRS}}(\text{CV}) = G I^2 (K \langle \beta_{\text{CVc}}^2 \rangle + \langle \beta_{\text{CV}}^2 \rangle) (N_{\text{CV}}^0 / (1 + K)) \quad (4)$$

below the cmc where $N_{\text{CV}}^{\text{m}} = 0$. This expression is similar to the one obtained for the HRS intensity of free CV in solution, but the slope of this curve is different. From the ratio of the experimental slopes, as seen from Figure 4, it yields

$$(K \langle \beta_{\text{CVc}}^2 \rangle + \langle \beta_{\text{CV}}^2 \rangle) / (1 + K) = 0.83 \langle \beta_{\text{CV}}^2 \rangle \quad (5)$$

This observation of a weaker slope in the presence of SDS in the solution indicates in particular that $\langle \beta_{\text{CV}}^2 \rangle$ is larger than $\langle \beta_{\text{CVc}}^2 \rangle$, irrespective of the value of K . In the limiting case, all the CV molecules enter a complex with one or more SDS molecules, this is a reasonable hypothesis since SDS is in excess at all concentrations of CV, and the hyperpolarizability ratio is $\langle \beta_{\text{CVc}}^2 \rangle / \langle \beta_{\text{CV}}^2 \rangle = 0.83$ as derived from eq 5. To further emphasize the changes undergone by CV upon interaction with SDS molecules, the experimental depolarization ratio was also determined and found to be $D = 0.89 \pm 0.02$ (see Figure 6). Such a value is no longer compatible with a pure octupolar symmetry for CV. This ratio is now in agreement with a more general planar C_{2v} symmetry. As a consequence, a quantitative analysis cannot be performed because different sets of the three independent nonvanishing elements of the hyperpolarizability tensor can lead to this depolarization ratio. The exact nature of the changes occurring in the molecular complexes of CV and SDS is therefore difficult to address, their origin being either a change in molecular symmetry or a change in the molecular structure or both simultaneously. The interaction with SDS surfactant molecules nevertheless yields a deviation of the CV symmetry from the pure octupolar symmetry toward a more dipolar symmetry.

For SDS concentrations above the cmc, micelles appear in the solution. The number density of CV molecules in interaction with the micelles is given by $N_{\text{CV}}^{\text{m}} = x N_{\text{m}}$, where N_{m} is the number density of micelles and x the number of CV molecules in interaction with one micelle. In all these experiments, the concentration of micelles is estimated to be 0.36 mM and therefore larger than that of CV, which is below 150 μM at all times. A probability distribution should be used for the number of CV molecules per micelle. For simplification, it is assumed that x is an average value. The HRS intensity at SDS concentrations above the cmc is then given by

$$I_{\text{HRS}}(\text{CV}) = G I^2 (x \sigma \langle \beta_{\text{CVm}}^2 \rangle + (1 - x \sigma) \langle \beta_{\text{CVc}}^2 \rangle) N_{\text{CV}}^0 \quad (6)$$

It is assumed that all CV molecules in solution are entering a molecular complex with one or more SDS molecules since the concentration of free SDS molecules also exceeds that of CV, namely $K \rightarrow \infty$. Also, $\sigma = N_{\text{m}} / N_{\text{CV}}^0$ and experimentally σ varies from 7.2 for a CV concentration of 50 μM down to 2.4 for a CV concentration of 150 μM . From the experimental slopes of the plots given above and below the SDS cmc in Figure 4

$$\langle \beta_{\text{CVm}}^2 \rangle = \frac{x \sigma - 0.17}{x \sigma} \langle \beta_{\text{CVc}}^2 \rangle \quad (7)$$

yielding in particular $\langle \beta_{\text{CVc}}^2 \rangle > \langle \beta_{\text{CVm}}^2 \rangle$. A trivial limiting case is $\langle \beta_{\text{CVm}}^2 \rangle = 0$, but this is unlikely given the value of the

hyperpolarizability $\langle \beta_{\text{CVc}}^2 \rangle$ of CV determined above. In that case, then $x = 0.17/\sigma$. In general, eq 7 therefore yields $x > 0.17/\sigma$. For instance, this latter inequality states that 7% at least of the micelles are in interaction with one CV molecule at an aqueous CV concentration of 150 μM . The exact value of the product $x \sigma$ though is unknown.

For the depolarization ratio, a value of $D = 0.79 \pm 0.02$ is obtained. The different value observed for D as compared to the two previous cases confirms that the interactions of CV with SDS break the initial pure octupolar symmetry in favor of the more general C_{2v} symmetry. Again, different sets of the elements of the hyperpolarizability tensor may yield such a value for the depolarization ratio precluding a more in-depth discussion of this interaction. It is however worth to note that despite the small amount of the micelles introduced in the solution, the changes are clearly observed although the data must be attributed to the overall system.

Conclusion

This experimental work presented here demonstrates that the interactions between probe molecules and micelles can be investigated at the molecular level, directly in solution, by the nonlinear optical technique of hyper-Rayleigh scattering. Unambiguous data including HRS intensity measurements as a function of the CV concentration for different SDS concentrations and polarization-resolved HRS measurements indicate that the interaction of CV molecules with SDS micelles can be distinguished from the interaction with freely dissolved SDS molecules. An in-depth discussion on the origins of the changes of the hyperpolarizability of CV, whether due to the change in symmetry or a change in the molecular structure, remains difficult hampered by a detailed knowledge of the multiplicity of the sets of elements of the hyperpolarizability tensor yielding the experimental data. However, the change of the CV molecular structure from a pure octupolar D_{3h} symmetry to a dipolar C_{2v} symmetry is clearly observed. This result does not allow a definite conclusion regarding the geometry of the association between CV and the micelles. HRS is nevertheless amenable to reveal these fine changes in the environment of the CV probe molecules.

References and Notes

- (1) Clays, K.; Hendrickx, E.; Verbiest, T.; Persoons, A. *Adv. Mater.* **1998**, *10*, 643.
- (2) Yokoyama, S.; Nakama, T.; Otomo, A.; Mashiko, S. *J. Am. Chem. Soc.* **2000**, *122*, 3174.
- (3) Mukhopadhyay, P.; Bhadraraj, P. K.; Savita, G.; Krishnan, A.; Das, P. K. *Chem. Commun.* **2000**, 1815.
- (4) Kauranen, M.; Verbiest, T.; Boutton, C.; Teerenstra, M. N.; Clays, K.; Scouten, A. J.; Nolte, R. J. M.; Persoons, A. *Science* **1995**, *270*, 966.
- (5) Wang, H.; Yan, E. C. Y.; Borguet, E.; Eisenthal, K. B. *Chem. Phys. Lett.* **1996**, *259*, 15.
- (6) Liu, Y.; Yan, E. C. Y.; Zhao, X.; Eisenthal, K. B. *Langmuir* **2001**, *17*, 2063.
- (7) Ghosh, S.; Krishnan, A.; Das, P. K.; Ramakrishnan, S. *J. Am. Chem. Soc.* **2002**, *125*, 1602.
- (8) Zyss, J.; Van, T. C.; Dhenaut, Ch.; Ledoux, I. *Chem. Phys.* **1993**, *177*, 281.
- (9) Clays, K.; Persoons, A. *Rev. Sci. Instrum.* **1994**, *65*, 2190.
- (10) Chui, T. W.; Wong, K. Y. *J. Chem. Phys.* **1998**, *109*, 1391.
- (11) Verbiest, T.; Clays, K.; Samyn, C.; Wolff, J.; Reinhoudt, D.; Persoons, A. *J. Am. Chem. Soc.* **1994**, *116*, 9320.
- (12) Vance, F. W.; Lemon, B. I.; Hupp, J. T. *J. Phys. Chem. B* **1998**, *102*, 10091.
- (13) Bersohn, R.; Pao, Y.; Frisch, H. L. *J. Chem. Phys.* **1966**, *44*, 3184.
- (14) Brasselet, S.; Zyss, J. *J. Opt. Soc. Am. B* **1998**, *15*, 257.
- (15) Myers, D. *Surfactant Science and Technology*; VCH Publishers: New York, 1992.
- (16) Joffe, M.; Yaron, D.; Silbey, R. J.; Zyss, J. *J. Chem. Phys.* **1992**, *97*, 5607.